Available online at www.sciencedirect.com
ScienceDirect
Geochimica et Cosmochimica Acta 73 (2009) 3795–3806
Geochimica et Cosmochimica Acta
www.elsevier.com/locate/gca

Low-temperature isotopic exchange in obsidian: Implications for diffusive mechanisms

Lawrence M. Anovitz [a,b,*], David R. Cole [b], Lee R. Riciputi [c]

[a] Department of Earth and Planetary Sciences, University of Tennessee, Knoxville, TN 37996, USA
[b] Chemical Sciences Division, MS 6110, P.O. Box 2008, Bldg. 4500S, Oak Ridge National Laboratory, Oak Ridge, TN 37831-6110, USA
[c] Chemistry Division, MS J514, P.O. Box 1663, Los Alamos National Laboratory, Los Alamos, NM 87545, USA

Received 8 January 2008; accepted in revised form 4 February 2009; available online 26 March 2009

Abstract

While a great deal is known about the interaction between water and rhyolitic glasses and melts at temperatures above the glass transition, the nature of this interaction at lower temperatures is much more poorly understood. This paper presents the results of a series of isotopic exchange experiments aimed at further elucidating this process and determining the extent to which a point-by-point analysis of the D/H or $^{18}O/^{18}O$ isotopic composition across the hydrated rim on a geological or archaeological obsidian sample can be used as a paleoclimatic monitor. Experiments were performed by first hydrating the glass for 5 days in water of one isotopic composition, followed by 5 days in water of a second composition. Because waters of near end-member compositions were used (nearly pure $^{1}H_2{}^{16}O$, $^{1}H_2{}^{18}O$, and $D_2{}^{16}O$), the relative migration of each species could be ascertained easily by depth-profiling using secondary ion mass spectrometry (SIMS). Results suggest that, during hydration, both the isotopic composition of the waters of hydration, as well as that of intrinsic water remaining from the initial formation of the glass vary dramatically, and a point-by-point analysis leading to paleoclimatic reconstruction is not feasible.

1. INTRODUCTION

The interaction of water with rhyolitic glasses and melts has long been of geologic interest, both in terms of how water effects the properties of magmas (Goranson, 1931; Tuttle and Bowen, 1958; Stolper, 1982a,b, 1989; Zhang et al., 1991, 1997a,b, 2003; Dingwell et al., 1996), and how obsidians weather (Anovitz et al., 1999, 2004, 2006a,b, 2008; Friedman and Smith, 1959, 1960; Riciputi et al., 2002). Obsidian hydration rates have been used as a chronometer (Friedman and Smith, 1959, 1960; Friedman et al., 1966, 1968; Friedman and Trembour, 1980, 1983; Ridings, 1996; Anovitz et al., 1999; Riciputi et al., 2002) and for analysis of paleoclimates (Anovitz et al., 2006b). It has also been suggested (Friedman et al., 1993a,b) that the isotopic compositions of hydrated volcanic glasses can be used to constrain ancient climatic conditions.

The use of obsidian hydration rates for archaeochronometry received a major new direction when Anovitz et al. (1999) suggested that the hydration profiles be measured using secondary ion mass spectrometry (SIMS) rather than the optical techniques traditionally used at that time. The success of the SIMS approach also suggested, however, that the isotopic approach to obsidian paleoclimatology (Friedman et al., 1993a,b) might be enhanced by analyzing changes in the stable isotopic composition across the hydration profile, rather than by analysis of the bulk-hydrated perlite. Friedman's approach relies on the fact that once the glass is fully hydrated, there is no driving force for diffusion. Thus, as long as the relative humidity of the

* Corresponding author. Address: Department of Earth and Planetary Sciences, University of Tennessee, Knoxville, TN 37996, USA. Fax: +1 865 574 4961.
E-mail address: anovitzlm@ornl.gov (L.M. Anovitz).

0016-7037/$ - see front matter © 2009 Elsevier Ltd. All rights reserved.
doi:10.1016/j.gca.2009.02.035

environment remains high, further isotopic exchange would, therefore, be stochastic and, likely, slow. If the water forming the perlite was structurally bound, this would further slow the process. In order to assess whether this approach would work at the scale of SIMS analysis, however, it was first necessary to determine whether the individual hydrogen and oxygen isotopes added to the glass during hydration remain fixed to a specific location in the glass, or whether they continue to move and exchange during further hydration. Such a phenomenon would require that the water react with the glass in such a way as to bind it strongly to the structure. This would be consistent, for instance, with the conclusion of Zhang et al. (1991) that hydroxyl groups, once formed, are no longer mobile, as long as such hydroxyls do not exchange with "matrix" water. Answering this question, in turn, requires a fundamental understanding of the nature of the hydration process under low-temperature conditions.

In order to test this question we have performed a series of two-part obsidian hydration experiments. In each, polished glass samples were first hydrated for 5 days in water of one isotopic composition (pure D_2O, for example), then for five more days in water of a different isotopic composition. In this way it was possible to determine whether the hydrogen or oxygen atoms that diffuse into the glass remained fixed during subsequent hydration, and thus to further elucidate the nature of the low-temperature hydration process.

The possible (end-member) results of these experiments are shown schematically in Fig. 1. Fig. 1A shows two profiles, the shallower representing the single-isotope profile after the first experiment, and the deeper the summed isotope profile after the second experiment. Fig. 1B shows the expected isotopic concentrations with depth in a case where the first isotopic species is strongly bound to the glass structure. In this case, that isotopic species, once locked in the glass structure, would not move from its initial position, and the second isotopic species would have to pass through it, bonding to the glass in the deeper parts of the structure. In this case the isotopic composition as a function of depth would reflect the temporal evolution of the isotopic composition of the external fluid. The second alternative (Fig. 1C) is for the case in which the first isotopic species is more weakly bound. In this case the first isotopic species can both exchange out of the glass with the second fluid, and move into deeper parts of the glass structure, being replaced in the shallower parts of the profile by the second isotopic species. In this case the isotopic profile does not directly represent changes in the isotopic composition of the external fluid with time. The purpose of the present experiments was to assess these alternatives.

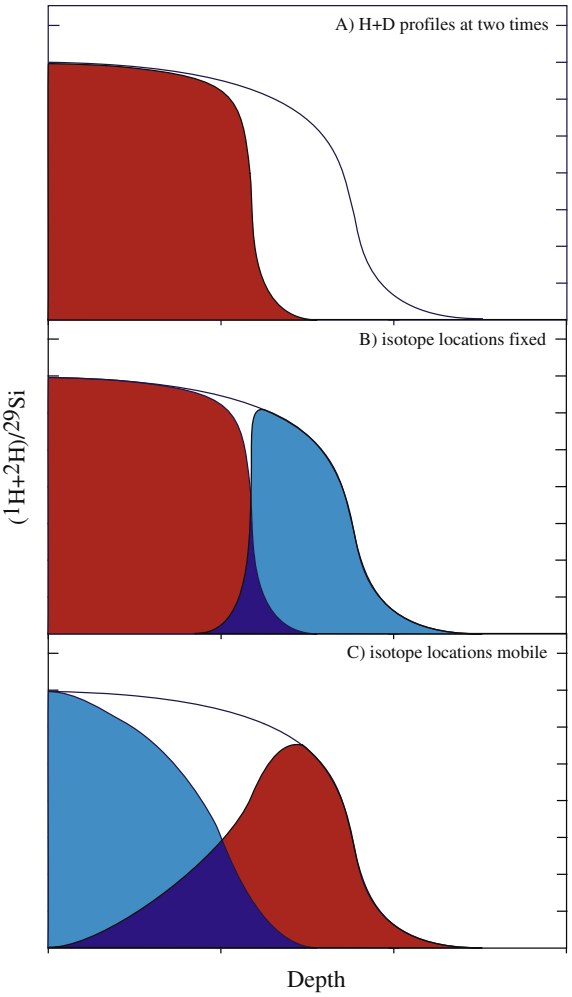

Fig. 1. Qualitative picture of possible results. (A) Total hydrogen plus deuterium profiles at two different times, representing the hydration profiles after the first and second parts of the two-part experiments reported here. The red indicates the integrated location of the isotope used for the first run after that run. (B) Case one, where the hydrogen/deuterium is strongly bonded so that the isotope added in the first run (red) remains fixed during the second run. The second isotope (blue), therefore, would pass through the first, and be concentrated in the deeper parts of the profile. (C) Case two, where the hydrogen/deuterium is weakly bonded to the glass structure. In this case, the isotope from the first run (red) is forced deeper into the glass, and some may be lost due to exchange with water outside the glass structure. The shallower parts of the profile are then dominated by the second isotope.

2. STARTING MATERIALS

All experiments were performed using obsidian from the Pachuca source, located in the Sierra Madre Oriental northeast of the Basin of Mexico. The geology and archaeology of the Pachuca source and the chemistry of the obsidian have been summarized by several authors (Holmes, 1900; García-Barcena, 1975; Lopez-Agilar et al., 1989; Cobean et al., 1991; Cruz, 1994; Cruz and Pastrana, 1994; Pastrana, 1996; Tenorio et al., 1998; Lighthart, 2001). The outcrops cover a large area near the town of Huasca, Hidalgo, and most of the mining was on the southern slopes of a mountain called Cruz del Milagro. Cobean et al. (1991) note that the Pachuca source "was probably the most important obsidian quarry in northern Mesoamerica during Prehispanic times". Optically the glass is green, and it shows a slight schiller in some directions due to microscopic vacuoles. The materials used for our experiments are essentially free of vacuoles and macroscopic ash inclusions, although a

few exist that were avoided during sample selection. Trace element data show that Pachuca obsidian is relatively rich in Mn, Zr, Hf and Cl, and relatively low in Ba relative to many other Mesoamerican obsidians.

Our experiments used small blocks of Pachuca obsidian 2–3 mm on a side polished on two parallel faces. The waters used included a distilled, deionized water obtained from a Barnstead NANOpure ion exchange ultrapure water system with a conductivity of approximately 18.3 M ohms prepared initially for isotopic exchange studies (water W1, $\delta D = -45.036‰$, $\delta^{18}O = -7.516$, Horita et al., 2002), a sample of nearly pure D_2O (99.26% D), and a sample of 95–98% pure $H_2{}^{18}O$ obtained from Cambridge Isotopes.

3. EXPERIMENTAL METHODS

The experimental and analytical techniques used in this study have been described elsewhere (Anovitz et al., 1999; Riciputi et al., 2002; Anovitz et al., 2004, 2006a,b). Thus, except for the method used for isotopic exchange, they will only be described briefly here.

Experiments were conducted in reaction vessels fabricated from VCR®-type vacuum fittings. To prepare the vessels, seals were polished and the vessels subsequently washed with water, acetone and ethanol, and baked dry at 150 °C. All experiments described herein were carried out at 150 °C, and initiated simultaneously. To do so, vessels were placed in a covered aluminum block containing wells for 10 vessels in a convection oven. Temperatures were monitored by three resistance temperature detectors (RTD's) inserted into tight-fitting wells in this block. Additional thermal mass for temperature stability was obtained by setting the aluminum block on a 2" thick steel plate.

Prior to assembly, sufficient water was placed in a Teflon cup seated in the vessel bottom to form a saturated two-phase liquid–vapor system at the temperature of interest. The amount used was small enough, however, that the samples on the mesh were suspended in the vapor phase, above the liquid water. This prevented direct contact between the steel and the liquid phase during the experiment and limited steel corrosion. As has been noted previously (Stevenson et al., 1989; Mazer et al., 1991), under these conditions the chemical potential of water at the surface of the glass remains identical to its value in the liquid, but the solubility of the glass in the vapor is several orders of magnitude less than in the liquid (Cohen, 1980; Lindsay, 1989 Fig. 7–30 for a summary). Thus, this experimental design allows diffusion to be studied independently from dissolution. The samples are then placed on the mesh, and the vessel sealed.

In our earlier studies it was determined that the initial heating time was relatively long if all 10 vessels at room temperature were placed simultaneously into an Al-block pre-heated to the experimental temperature. In order to increase the rate of heating, the vessels were first placed in boiling water (at $t = 0$ min) prior to insertion into the furnace, and the Al block was pre-heated to 170 °C. The beginning of each experiment was somewhat arbitrarily defined as the time at which the block/vessel assembly reached 148 °C. After the initial heating period temperatures recorded over the lifetime of the experiment varied by less than 0.5 °C. The experiments were terminated by removing the vessels from the block and quenching them in cold water. The total duration of the first run was 4 days, 20 h and 31 min, while the total duration of the second run was 4 days, 23 h, 53 min. After each vessel was quenched it was opened and the samples were placed in small plastic "freezer bottles" sealed with an *O*-ring and transferred as quickly as possible to a freezer at approximately −25 °C. All samples were stored in this freezer from the time of the experiment until the time of analysis in order to limit any changes during storage.

As the goal of these experiments was to use isotopic exchange to study the hydration of obsidian, most were performed in two steps. The first involved an initial 5-day hydration using one of the isotopically labeled waters described above. Several glass blocks were used in each experiment, and a period of 5 days was selected because previous experiments at this temperature had suggested that this would yield a reasonable hydration depth. After these first experiments were quenched, one block was removed from each vessel and stored for analysis. The remaining blocks were then hydrated for an additional 5 days using a second water whose isotopic composition was usually, but not always, different from the first. A summary of these runs is given in Table 1.

4. ANALYTICAL TECHNIQUES

To prepare samples for SIMS analysis, 5 to 6 holes were drilled in 1 in. diameter, 3/8 inch thick aluminum disks. Epoxy was used to mount the obsidian samples in these holes with the hydrated surface exposed. A sample of freshly polished Pachuca obsidian was also mounted in each disk to (a) ensure the availability of a flat surface to aid with calibrating sputter depths (see below) and (b) provide an internal standard. The finished disks were coated with a thin layer of gold to provide surface conductivity. To minimize the presence of adsorbed water, samples were baked at 45 °C for 12–18 h before introduction into the vacuum system of the ion microprobe, which occurred a minimum of 12 h before analysis. As shown previously (Riciputi et al., 2002) these steps result in minimization of adsorbed water prior to analysis without significantly effecting the profile.

The distributions of hydrogen (^1H), deuterium (^2H), ^{18}O, and ^{29}Si as a function of depth were measured using a Cameca 4f secondary ion mass spectrometer. The SIMS technique utilizes a focused, mass-selected beam of primary ions accelerated to sputter the surface of the obsidian. For these analyses, negatively-charged, ^{16}O primary ions were accelerated at 12.5 keV. The primary beam, with a diameter of 50 μm and a current of 130 nA, was rastered over an area of 150 μm^2. This has been shown (Riciputi et al., 2002) to produce well-shaped craters with flat bottoms. Positively charged secondary ions with 80 ± 20 eV of excess kinetic energy were analyzed. This energy offset permitted analysis of ^{18}O using an oxygen beam, but not ^{16}O. Use of the 150 μm diameter transfer lens and a 400 μm diameter field

Table 1
Oxygen and hydrogen profile characteristics for each experiment.

Run time days	Water used		H	H + D	H + D half-fall		^{18}O		
	Run 1	Run 2	Background	Surface	Concentration	Depth (nm)	Half-fall concentration	Half-fall depth (nm)	Integrated
10	D_2O	$H_2{}^{18}O$	0.0408	0.6000	0.3204	2.5983	0.00294	0.465	0.003805
10	D_2O	D_2O	0.0432	0.5600	0.3016	2.7914			
10	D_2O	W1	0.0427	0.6100	0.3264	2.6426			
10	W1	D_2O	0.0471	0.5580	0.3025	2.7199			
5	D_2O	–	0.0274	0.5800	0.3037	2.2001			
5	W1	–	0.0404	0.6020	0.3212	2.0007			
5	$H_2{}^{18}O$	–	0.0420	0.6020	0.3220	1.9517	0.00709	0.550	0.009574
10	W1	$H_2{}^{18}O$	0.0422	0.5530	0.3126	2.7999	0.00609	0.550	0.009114

Depths are in microns, concentrations in $(H + D)/^{29}Si$.
Half-fall concentrations and depths for ^{18}O are based only on the main part of the fitted profile, not on the two near-surface fits or the profile as a whole.

aperture restricts transmission so that only ions from the central 33 μm of the sputter crater are transmitted through the secondary mass spectrometer. Selected masses were analyzed by cycling the secondary ion magnet through the masses of interest. Secondary ion signals were monitored using an electron multiplier, with count times of 1–3 s per cycle per element of interest. The intensity of ^{29}Si was used as a reference species to correct for variations in secondary ion intensities due to changes in primary ion beam intensity between different analyses.

Crater depths were measured using a Tencor Alpha-Step 200 profilometer. For most samples, the craters are very regular in shape with wide, flat, bottoms, indicating that depth resolution was optimized during the analysis. Repeated depth measurements on craters sputtered on flat samples indicate that reproducibility of the depth measurement is better than 3%.

Comparison of hydrogen and deuterium fluxes in each experimental run product is complicated by the fact that the ionization efficiencies of hydrogen and deuterium are not identical. Thus, equal $^1H/^{29}Si$ and $^2H/^{29}Si$ count ratios do not necessarily imply equal hydrogen and deuterium concentrations. To correct for this, and to allow total $^1H + ^2H$ profiles to be obtained, a correction factor had to be determined. This was obtained by assuming that the maximum concentrations of ^1H and ^2H will be identical in two, single-isotope experiments run for equal lengths of time. That is, the equilibrium saturation concentrations are not isotope-dependent. The results of this assumption/correction are shown in Fig. 2, which shows the original and corrected 5- and 10- day deuterium profiles in comparison to hydrogen profiles run for identical times. It should be noted, however, that while the derived correction factor, 2.57, allows direct comparisons to be made between deuterium and hydrogen data, it does not yield an actual concentration for either isotope.

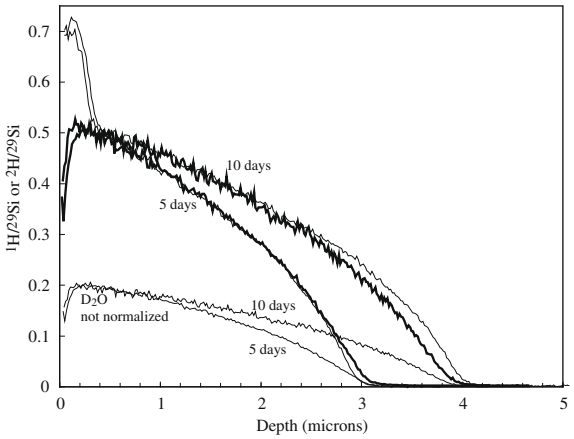

Fig. 2. Original and corrected 5- and 10-day deuterium profiles compared to hydrogen profiles run for identical times, showing the effect of correction for differential ionization efficiencies. Heavy lines: normalized D_2O values.

5. RESULTS AND DISCUSSION

5.1. Hydrogen-deuterium diffusion and exchange

Hydrogen and deuterium depth profiles measured in the experimental products are shown in Figs. 3–5. The data making up the profiles are provided in the electronic annex. It is apparent from these figures that neither the H_2O nor the D_2O profiles remain constant when the second isotopically labeled "water" diffuses into the glass. Comparison of results in Figs. 4A and B with Fig. 5C, or Fig. 3B with Figs. 5A and B indicates that, if D_2O is diffused into the glass for 5 days following an initial 5 days of H_2O hydration, or if H_2O is diffused into the glass for 5 days following an initial 5 days of D_2O hydration, the profiles of the material initially diffused into the glass no longer match those seen after the initial 5 days. Rather, they appear to have been displaced by the addition of the latter species. This is true not only of the H_2O or D_2O initially diffused in at low temperatures during the first part of each experiment, but of the hydrogen initially in the glass as well. This "intrinsic water" was probably locked into the glass during its quench from the melt. In experiments in which only D_2O was added to the glass (Figs. 4A and 5C), the intrinsic hydrogen content is lower than its initial value (the value beyond the diffusion profile) over most of the hydrated zone, but tends to "pile-up" and is at larger-than-initial values in the deepest part of

the hydrated rim. This behavior is also manifested as a small hump in the hydrogen profiles in which H_2O was also added to the glass (Figs. 4B and C). Thus it appears clear that neither intrinsic nor diffusion-derived water remains fixed in place as additional water is added during diffusion (Case C, Fig. 1).

These results also imply that, as hydration progresses, the hydrogen isotope ratios at any point in the glass are constantly changing if the exterior isotopic values change, and that isotopic profiles in the glass do not directly represent changing isotopic ratios in the exterior fluid with time (although it might be possible to deconvolute such results). Similarly, even if the diffusion-derived water were to be somehow removed, the isotopic composition of the intrinsic water no longer represents the initial isotopic concentration of the high-temperature quenched glass. Therefore, since high-temperature partitioning studies (Stolper, 1982b) suggest that this intrinsic water is likely present mostly as hydroxyl groups bound to the glass structure, a result consistent with our own FTIR analyses of these materials (Anovitz et al., 2008), our experiments show that even relatively tightly-bound hydroxyl groups are not exempt from isotopic exchange with later hydration waters.

Thus, water that enters the glass remains isotopically mobile, regardless of whether that water is present as molecular water, the likely species entering at low temperatures (Anovitz et al., 2008), or as hydroxyl groups. This could imply that, at least in Pachuca obsidian, both molecular water and hydroxyl groups are mobile, even at relatively low temperatures. It is more likely, however, that the isotopic composition of the intrinsic hydroxyl groups is being modified by exchange with the diffusion-derived molecular water. The hydrogen from the intrinsic hydroxyl groups then moves down the chemical potential gradient into the glass, causing the apparent "pile-up" at the diffusion front.

5.1.1. Quantitative evaluations

In addition to the individual hydrogen and deuterium depth profiles, Figs. 3–6 also show the concentration of hydrogen plus deuterium as a function of depth. In those experiments in which two isotopes diffused into the glass, the summed profile is nearly identical both in shape and depth to profiles in which only a single isotope was used. This behavior is consistent with results reported previously (Anovitz et al., 2008) that, under these conditions, there appears to be little observable difference between the diffusion rates of H_2O and D_2O in Pachuca obsidian.

We can quantify these results by characterizing each profile with a half-fall depth. As we have demonstrated in our previous work (Riciputi et al., 2002; Anovitz et al., 2004), the depth of the diffusion profile can be conveniently represented in terms of one of several "characteristic depths" that characterize the profile as a single point. This point can be any value, such as the half-fall distance or the distance to the inflection point, that is consistently identifiable for any profile of interest, and can be converted into a characteristic diffusion coefficient as:

$$D_{CH} = \frac{x_{HF}^2}{t} \quad (1)$$

Although we have shown experimentally that the half-fall depth does not quite follow the simple square-root-of-time dependence implied by this equation (Anovitz et al., 2006b), its use is consistent with our previous studies (Anovitz et al., 1999; Riciputi et al., 2002; Anovitz et al., 2004, 2006a,b; Anovitz et al., 2008) and it provides a convenient method of characterizing and comparing hydration depths. The half-fall depth used in these calculations is defined as the depth at which the concentration is equal to the average of the background and maximum concentrations. Half-fall depths for the profiles shown in Figs. 3–6 are listed in Table 1. As can be seen, the half-fall depths and concentrations within both the 5- and 10-day experimental sets are remarkably similar, yielding averaged half-fall depths for the hydrogen profiles of 2.05 ± 0.13 μm at 5 days and 2.71 ± 0.09 μm at 10 days, and essentially identical half-fall concentrations of $(^1H + {}^2H/{}^{29}Si)$ of 0.32 ± 0.01 at 5 days and 0.31 ± 0.01 at 10 days (standard deviations are given as 1σ). By comparison, the half-fall depths predicted by our previous work on Pachuca obsidian (Anovitz et al., 2006b) for the 5- and 10-day runs, 2.16 ± 0.03 and 2.91 ± 0.03 μm (1σ) are slightly higher, but in reasonable agreement at the 2σ level, especially as the data from the present paper contain both hydrogen and deuterium data and those of Anovitz et al. (2006b) do not.

Table 2 shows the integrated water and deuterium concentrations, as appropriate, for both the first and second hydrations, the hydrogen plus deuterium curve and, where possible, for the intrinsic water (all in units of counts/

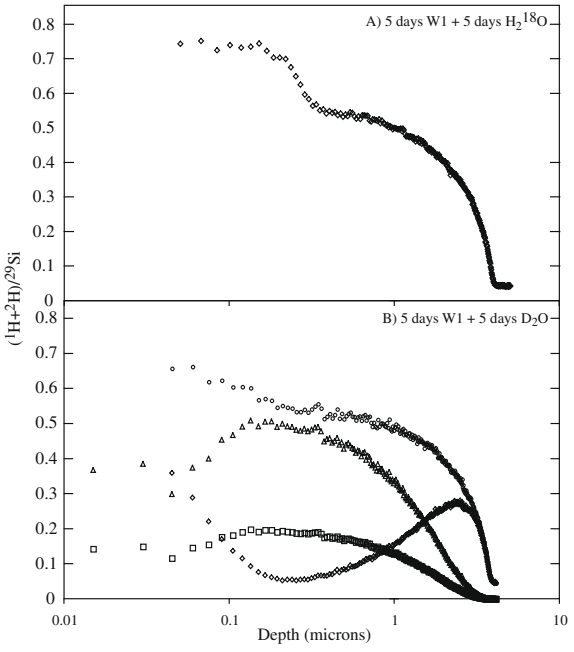

Fig. 3. Ten-day isotope exchange experiments in which water W1 was used for the first 5 days of the experiment. Squares: uncorrected $D/^{29}Si$, Triangles: corrected $D/^{29}Si$, Diamonds $H/^{29}Si$, Circles: $(H + D)/^{29}Si$. (A) Five days in water W1 followed by 5 days in $H_2{}^{18}O$. (B) Five days in water W1 followed by 5 days in D_2O. All experiments were conducted at 150 °C at a pressure on the liquid–vapor curve.

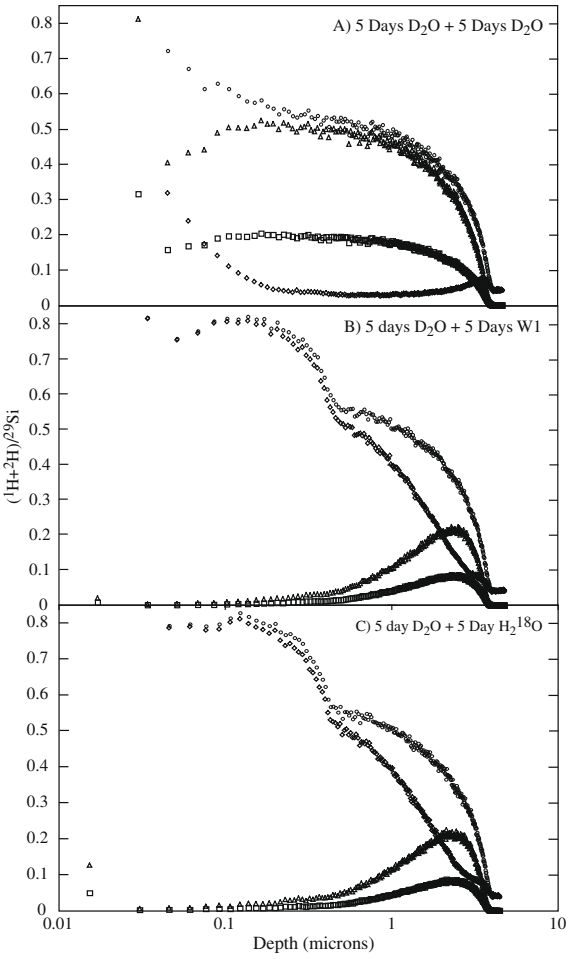

Fig. 4. Ten-day isotope exchange experiments in which D_2O was used for the first 5 days of the experiment. Squares: uncorrected $D/^{29}Si$, Triangles: corrected $D/^{29}Si$, Diamonds $H/^{29}Si$, Circles: $(H + D)/^{29}Si$. (A) Five days in D_2O followed by a second 5 days in D_2O. (B) Five days in D_2O followed by 5 days in water W1. (C) Five days in D_2O followed by 5 days in $H_2{}^{18}O$. All experiments were conducted at 150 °C at a pressure on the liquid–vapor curve.

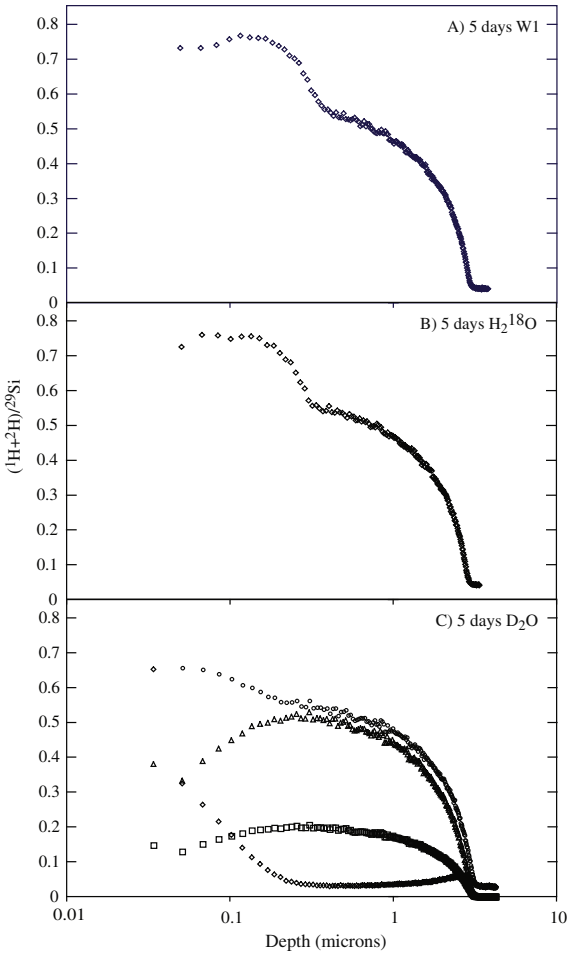

Fig. 5. Five-day, single-isotope experiments. Squares: uncorrected $D/^{29}Si$, Triangles: corrected $D/^{29}Si$, Diamonds $H/^{29}Si$, Circles: $(H+D)/^{29}Si$. (A) Five days in water W1. (B) Five days in water $H_2{}^{18}O$. (C) Five days in D_2O. All experiments were conducted at 150 °C at a pressure on the liquid–vapor curve.

counts ^{29}Si, with ^{2}H values corrected for ionization efficiency as described above). Data are given both with and without corrections for the near-surface features described below. These corrections were made by projecting the data linearly from beyond the surface features to zero depth, and using this curve to integrate the near-surface region of the profile instead of the measured near-surface values. As can be seen in Table 2, in many cases this correction was relatively small.

The first feature that is apparent when examining the integrated concentrations is that not all of the water diffused into the glass in the first run is retained in the second. The average integrated hydrogen isotope contents of the 5 day D_2O and W1 runs, with or without a surface correction, is 1.03 ± 0.02. In all cases in which a different isotopic fluid was run in the second 5-day cycle, the integrated content of the first isotope after the second experiment was significantly reduced. These experiments yield an average integrated concentration of the first isotope of 0.52 ± 0.02. Thus almost half of the first isotope diffused out of the glass during the second part of the hydration experiment.

As described above, the two experiments in which only D_2O was used allow examination of the behavior of intrinsic water during hydration. This is because intrinsic water contains the low terrestrial deuterium content common in natural waters. Unfortunately, because the overall integrated concentrations are relatively low the relative effects of profile changes in the near-surface are relatively large. Thus, on a percentage basis, these values are less accurate. The average intrinsic hydrogen isotope concentrations in these two profiles are 0.04 $^{1}H/^{29}Si$ and 4E-5 $^{2}H/^{29}Si$. Subtracting this initial value from each point of the surface-uncorrected profile and integrating yields small positive values, as expected from the obvious water addition in the near-surface portions of each profile (Table 2). Repeating this procedure using surface-corrected profiles yields a slight gain at 5 days, and a slight loss after 10 days. This is well within the expected uncertainty in the surface-correction procedure, and thus it is unclear whether the bulk

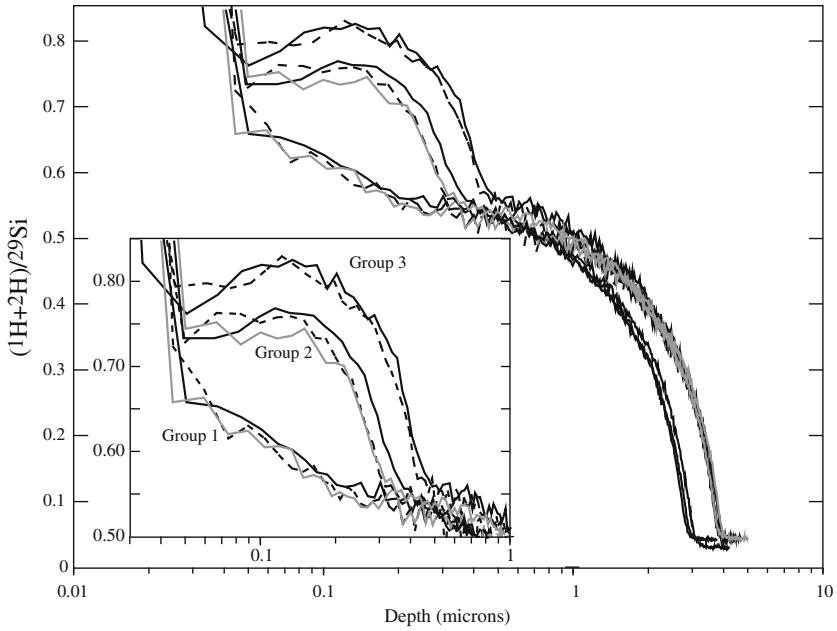

Fig. 6. Summary of H_2O/D_2O exchange experiments, showing details of variations in near-surface behavior. Group 1 (shallowest surface profiles): solid – 5 day D_2O, dashed – 10 day D_2O, grey – 5 day W1 followed by 5 day D_2O. Group 2 (intermediate depth surface profiles): solid – 5 day W1, dashed – 5 day $H_2{}^{18}O$, grey – 10 day W1. Group 3 (deepest surface profiles): solid – 5 day D_2O followed by 5 day W1, dashed – 5 day D_2O followed by 5 day $H_2{}^{18}O$.

hydrogen isotopic concentration of intrinsic water in the glass can be changed during subsequent hydration, although it clearly changes on a point-by-point basis.

These data have important implications for our understanding of the mobility of waters of hydration in obsidian under these conditions. As was also implied by the profile shapes, it is clear that both waters of hydration and intrinsic waters are very mobile. Not only are the hydrogen or deuterium atoms from water that initially diffused into the glass forced deeper by addition of later water, but earlier-diffused isotopic species also clearly exchange with water outside of the glass itself. In addition, even intrinsic hydroxyl groups, those initially in the glass prior to low-temperature hydration, exchange with water added during hydration. If this sort of exchange occurs in days at 150 °C, it is reasonable to assume that it occurs more rapidly at higher temperatures and therefore the isotopic compositions of hydroxyl groups at high temperatures are not fixed, even if the hydroxyl groups themselves do not diffuse. In addition, isotopic exchange between diffusing water and intrinsic hydroxyls may also occur over modest periods of geologic time under ambient conditions, although the temperature dependence of this process is, as yet, unknown.

5.1.2. Near-surface effects

While profiles deeper than approximately 0.5 μm all show the *s*-shape commonly observed in hydrated obsidians, the portions of the profiles nearer the surface show a rather different geometry (cf. Anovitz et al., 1999). Despite the potential distortion of the near-surface profiles due to ion-bean energetics, there are a number of consistencies in the features of both the summed ($^1H + {}^2H$) profile, and

Table 2
Integrated values for hydrogen isotope concentrations for each experimental profile.

Run Time days	Water Used		1st isotope integrated		2nd isotope integrated		Intrinsic ^1H integrated		Total H + D integrated	
	Run 1	Run 2	Surface correc.	Not surface correc.	Surface correc.	Not surface correc.	Surface correc.	Not surface correc.	Surface correc.	Not surface correc.
10	D_2O	$H_2{}^{18}O$		0.5019	0.8327	0.8859			0.8327	1.3879
10	D_2O	D_2O			1.3083	1.2822	−0.0081	0.0411	1.3003	1.3233
10	D_2O	W1		0.5006	0.8519	0.9007			0.8519	1.4013
10	W1		0.5171	0.5538	0.7480	0.7183			1.2652	1.2721
5	D_2O	–	1.0525	1.0067			0.0382	0.0809	1.0907	1.0876
5	W1	–	1.0118	1.0461					1.0118	1.0461
5	$H_2{}^{18}O$	–	0.9107	1.1543					0.9107	1.1543
10	W1	$H_2{}^{18}O$	1.3545	1.3858					1.3545	1.3858

its individual (^1H and ^2H) components that may be assessed. As can been seen in Fig. 6, both the 5-day and 10-day profiles fall into three groups. The first, exhibiting the shallowest near-surface effect, comprises the 5 day D_2O run and the two experiments in which the second run used D_2O. In each case deviation from the *s*-shaped profile begins at a depth of about 0.25 μm, and consists of a single, error-function-like addition to the main profile. The second group is represented by one experiment in which H_2O was used for both runs, and two in which either H_2O (W1) or $H_2{}^{18}O$, was run for 5 days. In these experiments the near-surface effect is deeper, beginning at about 0.35–0.4 μm, and there is a region of constant, or slightly declining concentration from about 0.15 μm depth toward the surface. The third group consists of two 10-day experiments in which D_2O was run for the first 5 days, and either W1 or $H_2{}^{18}O$ for the second 5 days. The near-surface profiles in these samples are essentially identical in shape to those of group two, but reach a higher near-surface maximum concentration and extend deeper into the sample, beginning at 0.45–0.5 μm. In fact, the shapes of these regions for both the second and third groups look much like that of the overall profile – but narrower and with a higher projected surface concentration.

One possible explanation for the observed near-surface phenomena is post-experimental D/H exchange. In all three groups the near-surface increase reflects increases in the hydrogen concentration. Deuterium, by contrast, always drops near the surface regardless of whether it was used in the entire experiment, or only in the second run. The depth at which this decrease is detected, approximately 0.15–0.25 μm, is similar to that of the error-function-like increase in the overall profile in the first group, and the near-constant section in the second and third sets. This flattening cannot be solely due to post-experimental effects, however, because it was also observed: (a) in the 10-day experiments in which no D_2O was used, and (b) in experiments where D_2O was only used for the first 5 days. In both cases the concentration of D_2O in the near-surface at the end of the experiment was very low, and thus a significant D_2O/H_2O exchange is not possible. In fact, the only three experiments in which the near-surface downturn in D_2O can affect the shape of the near-surface curve are in group one. Even in that group, however, if the near-surface behavior was due solely to D/H exchange, then the summed curve should be flat, which it is not.

A second near-surface feature is observed in the deuterium profiles in experiments where 5 days of hydration with D_2O was followed by 5 days of hydration with W1 or $H_2{}^{18}O$. In both cases the D_2O profile does not decrease monotonically from its interior maximum towards the surface, but shows a slight "bump" near 0.25 μm depth. As can be seen more clearly in Fig. 7, this may, in fact, represent a change in the slope of the D_2O depth profile at about 0.45 μm depth. This correlates reasonably well with the boundary between the two sections of the overall profile, suggesting this is another part of the same feature.

In two of the group-one experiments the glass was only exposed to D_2O. Nonetheless, both show an error-function-like near-surface feature that is primarily caused by an increase in H_2O, rather than D_2O. Thus, this part of the profile can neither have formed during the experiment itself, nor during quenching while the vessel remained sealed. Either this water must have come from the initial, intrinsic water in the glass, which is primarily H_2O, or this part of the profile must have formed after the experiment. Fitting the hydrogen in this part of the profile using the rate equation of Anovitz et al. (2006b) to derive diffusion coefficients yields a half-fall distance of 0.071 μm, and background and surface $^1H/^{29}Si$ concentrations of 0.03 and 0.50, respectively. Extrapolation of the experimental data to 25 °C yields a diffusion coefficient of 1.28E-09 $\mu m^2/s$. For this diffusion rate at this temperature the group-one near-surface profile would have required 44.5 days to form, clearly suggesting that this part of the profile was not produced by post-experimental exchange. Similarly, integration of the hydrogen profile suggests that the surface section comprises an addition of water to that initially in the glass, and thus it is unlikely that this results from redistribution of the intrinsic water. The possible origins of this feature will be discussed further below.

5.1.3. H/D ratios

Fig. 8 shows the H/D ratios in the five experiments in which D_2O was used. As expected, the H/D profiles for the two experiments in which D_2O was run for 5 days, followed by either H_2O or $H_2{}^{18}O$ for 5 days are nearly identical. Similarly, the profile shapes of the 5- and 10-day runs are also essentially identical, although the 10-day profile is understandably deeper. All three experiments in which D_2O was the second fluid show a nearly identical decrease in the first ~0.2 μm of the profile. In the 10-day run in which D_2O was run after H_2O, however, D_2O penetrates less deeply, and the background H/D value is achieved at shallower depths compared to experiments in which D_2O was run in the first part of the experiment. However, the half-fall distances for these two runs differ by only 0.07 μm (Table 1). Conversely, background H/D values are achieved at a greater depth in this run than in that in which D_2O was run for 5 days alone. This latter observation probably reflects the increase in the diffusion coefficient for water caused by the initial hydration of the glass, allowing D_2O to penetrate that glass more deeply after 5 days in one experiment than in the other. As was noted above, however, it is also apparent that once D_2O has entered the glass it continues to penetrate further during later hydration with H_2O.

5.2. Oxygen diffusion and exchange

The constraints involved in interpreting oxygen isotope exchange profiles are different from those involved with hydrogen and deuterium. As pointed out by Doremus (1995, 1996, 1998a,b), an oxygen atom entering a glass matrix as part of a water molecule is surrounded by a large number of oxygen atoms with which it can exchange. Thus, if the two oxygen populations (water and glass) are free to exchange, oxygen in the water molecule can undergo partial or complete isotopic equilibration with the glass while the

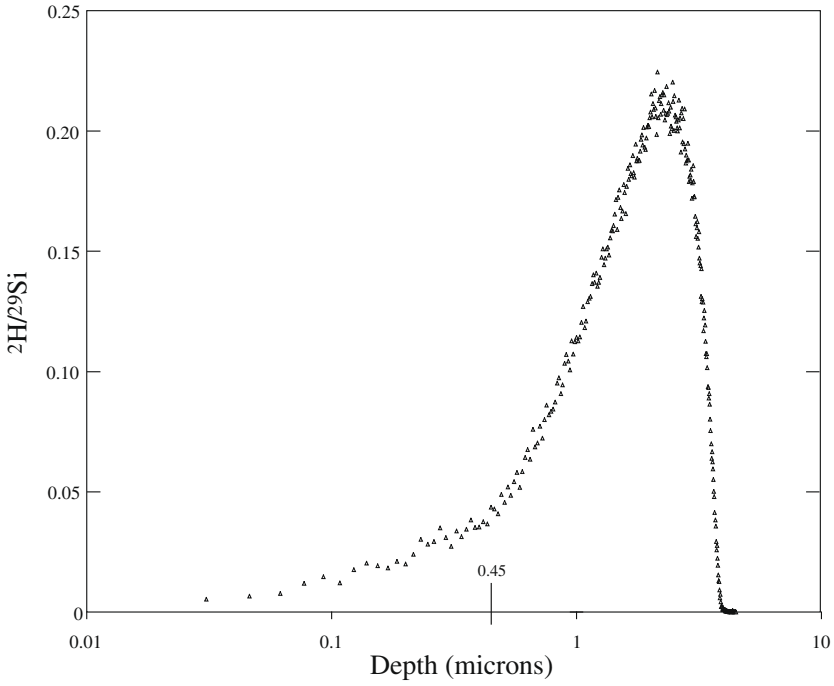

Fig. 7. Intensity-corrected D_2O depth profile for the experiment run for 5 days in D_2O followed by 5 days in $H_2{}^{18}O$. Note the change in slope in the profile near 0.45 μm.

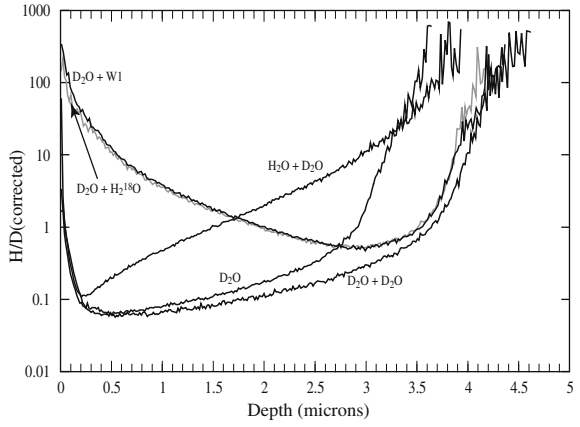

Fig. 8. H/D ratios in the five experiments in which D_2O was used. Each curve is labeled with the fluid used for each half of the reaction in the order in which they were run.

water molecule itself continues to diffuse. Thus the oxygen profile may appear to be significantly shallower than the accompanying hydrogen or deuterium profile.

Three experiments conducted with $H_2{}^{18}O$ allow examination of the diffusion of water into the glass matrix. In the first, $H_2{}^{18}O$ was run for 5 days, in the second, 5 days of $H_2{}^{18}O$ followed an initial 5 days of W1, and in the third, 5 days of $H_2{}^{18}O$ followed an initial 5 days of D_2O. These three profiles are shown in Fig. 9 as a function of $\log_{10}$ distance, which more clearly shows details near the surface. In all three cases, most of the profile can be fit with a simple error function, and the calculated $^{18}O/^{29}Si$ diffusion coefficients based on the half-fall distances are nearly identical (7.0E-7 $\mu m^2/s$, 7.0E-7 $\mu m^2/s$, and 5.0E-7 $\mu m^2/s$, respectively), although the surface value of the $D_2O + H_2{}^{18}O$ experiment is significantly smaller (surface $^{18}O/^{29}Si$ values of 0.014, 0.012 and 0.0057, respectively). As with the ^1H and ^2H profiles, however, all of these profiles show a deviation from a simple error function near the surface. This portion of each curve can be fitted as the sum of two additional error functions with different surface concentrations and diffusion coefficients. In the case of the 10-day runs, the surface concentrations of the second additional error functions are identical to that of the first (deepest), while in the 5-day run this function has a slightly lower value (0.008). The surface values for the third error functions (5 day $H_2{}^{18}O = 0.04$, 10 day $(H_2O + H_2{}^{18}O) = 0.06$, 10 day $(D_2O + H_2{}^{18}O) = 0.024$) vary somewhat, with the value for the $D_2O + H_2{}^{18}O$ experiment again being the smallest. The diffusion coefficients (calculated at 150 °C) for all three runs calculated from the second (all equal to 4.0E-8 $\mu m^2/s$) and third (all equal to 1.0E-9 $\mu m^2/s$) error functions are remarkably similar, although they require slightly different surface values. As can be seen from the surface compositions described above, however, and from the integrated values in Table 1, the overall amount of ^{18}O added in the 10-day run after D_2O (part of hydrogen profile group three) was decidedly less that added in the other two runs, which fall in hydrogen profile group two.

The depths of the near-surface regions in the ^{18}O profiles are also remarkably similar to those observed in the hydrogen profiles. In all three cases the second error function reaches one percent contribution to the overall concentration at a depth of about 0.5 μm. This suggests that the oxy-

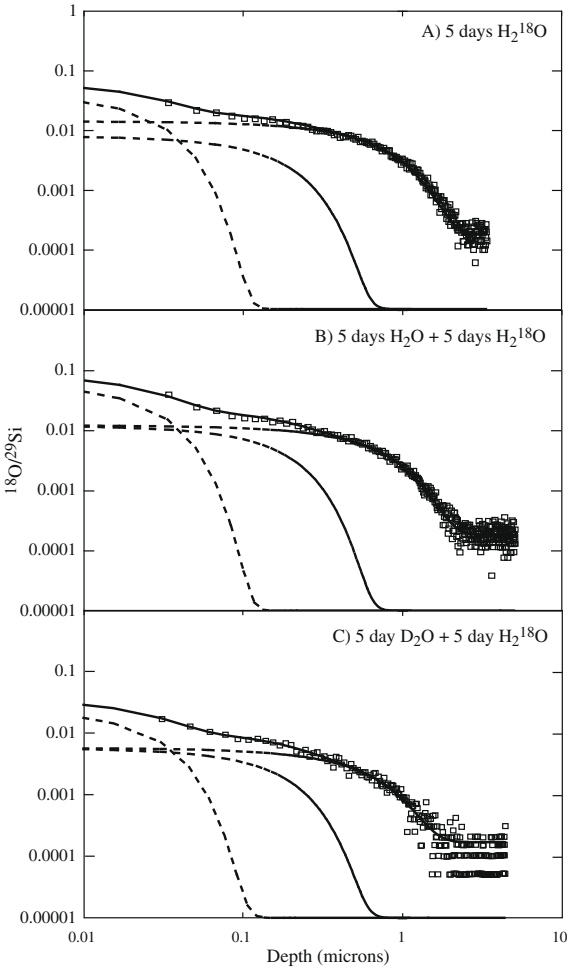

Fig. 9. ^{18}O profiles for experiments using $H_2{}^{18}O$. (A) Five day $H_2{}^{18}O$. (B) Five days W1 + 5 days $H_2{}^{18}O$. (C) Five days D_2O + 5 days $H_2{}^{18}O$. Solid lines are calculated ^{18}O profiles, dashed lines are the three pieces of the fitting equations. Note that the apparent parallel data sets at larger depths and lower concentrations in figure C are due to the analytical precision, and appear separate due to the log concentration scale.

gen exchange between the diffusing water and the glass matrix (Doremus, 1995, 1996, 1998a,b) has probably reached equilibrium in the near-surface. Thus the near-surface sections of each profile represent further addition of water that underwent little oxygen exchange with the matrix.

As with the hydrogen and deuterium data, it is reasonable to ask whether the near-surface phenomena might be due to exchange after the experiment, thereby explaining the features fitted by the second and third error functions. This would imply that the solubility increases with decreasing temperature in a manner not observed in our experiments to date, but such an effect should, nonetheless, be considered. If we use the equation for half-fall depth as a function of time and temperature derived from our hydration experiments on Pachuca obsidian (Anovitz et al., 2006b) we find that at 25 °C the shallowest profile (part three, $x_{ch} = 0.021$ μm for the 5-day $H_2{}^{18}O$ experiment) would require 2.5 days to form. As noted for the hydrogen data, the deeper parts of this profile would require even longer to form, as would any changes occurring during refrigeration. This again suggests that a post-experimental exchange mechanism is an unlikely explanation for even this shallowest part of the observed profile. It is also unclear why such a profile would form under such conditions. Exchange of hydrogen for deuterium or H_2O for D_2O might occur, but it is unclear why the total hydrogen plus deuterium or the ^{18}O content should increase under such a scenario.

One possible explanation for part of these phenomena for both oxygen and hydrogen is that these analyses were obtained using a relatively large beam-current. The absolute depth of this part of the profile might, therefore, have been artificially increased due to knock-on during SIMS analysis. Two studies (Lovell et al., 1999; Richardson et al., 2001) suggest, on the basis of neutron reflectometry, that there is a narrow (approximately 50 Å thick) surface layer in hydrated plate glass. This layer is water-rich relative to the rest of the profile, forms relatively rapidly, and does not increase in thickness with time. It is possible, therefore, that, at least for this narrowest part of the profile, the observed depth has been artificially increased due to knock-on phenomena. The actual depth of this effect, in the 0.01–0.02 μm range is, however, too small to significantly affect the rest of the profile, and is unlikely to differentially affect the near-surface profiles of the three groups discussed above.

Fig. 10 shows the hydrogen to oxygen ratio as a function of depth for the 5-day $H_2{}^{18}O$ experiment. The $H/^{18}O$ ratio increases steadily with depth (with a small possible offset at the limit of the near-surface added hydrogen profile at about 0.3 μm) to approximately the depth at which the oxygen profile reaches background (about 2.2 μm). The curve then decreases due to a decrease in hydrogen concentration. This curve reflects the exchange of ^{18}O into the glass matrix. The continuous rise with depth reflects the growing depletion of ^{18}O relative to that originating with the hydrogen as ^{18}O exchanges with ^{16}O in the glass matrix. The drop in the deeper parts of the profile is due to the fact that the ^{18}O profile is shallower than the accompanying hydrogen profile.

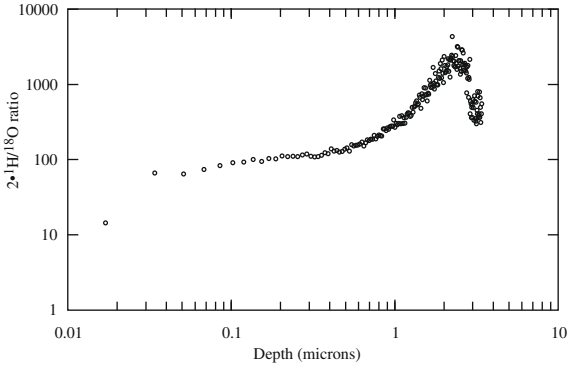

Fig. 10. Hydrogen to oxygen ratio in the hydration profile of the experiment run for 5 days in $H_2{}^{18}O$. Data are plotted as $2 \cdot {}^1H/{}^{18}O$.

6. CONCLUSION

The goal of these experiments was to test whether hydrogen isotopes diffused into obsidian at relatively low temperatures become so strongly bound to their initial sites that they remain in place during subsequent hydration. The results of our experiments clearly show that this is not the case. Not only are isotopic profiles subject to change during hydration, but even the overall isotopic content of the glass changes due to exchange between the water in the glass and external water.

In their work on isotopic exchange in volcanic glass Friedman et al. (1993a,b) suggested that the D/H ratios in hydrated obsidians could be used to monitor paleoclimatic conditions. They suggested that, once the glass is fully hydrated little or no isotopic exchange occurs with the environment. They based this on field comparisons of results from adjacent ash beds of different ages, which appeared to retain different isotopic signatures. In addition, they found that samples of the Lava Creek ash (erupted 0.61 Ma) collected from a number of sites in the western and central United States were in distinct isotopic disequilibium with modern local waters. This conclusion is not, in fact, unreasonable, as the driving force for diffusion by hydration, the chemical potential gradient, disappears once the sample is fully hydrated. Further isotopic exchange will then occur only by stochastic processes, and is likely to be much slower as there is no chemical potential gradient to drive them. While the absolute rate of such an exchange will not, however, be zero, its magnitude cannot be determined from either Friedman et al.'s (1993a,b) data or our own.

It is, however, clear from our study that extension of Friedman et al.'s (1993a,b) technique to SIMS microanalysis of hydrated rims on obsidian samples is untenable. Our data clearly show that exchange during hydration of an incompletely hydrated sample both modifies the point-by-point isotopic composition of the sample, and the isotopic composition of the hydrated rim as a whole. The latter occurs not only as a function of dilution by infiltrating water, but due to loss of isotopic components from the hydrated rim to the environment. Thus isotopic paleoclimatology based on hydrated glasses would appear to be limited, at best, to fully hydrated materials.

ACKNOWLEDGMENTS

Research sponsored by the Archaeometry Program, National Science Foundation grant numbers SBR-98-04350, and BCS-0108956, and by the Division of Chemical Sciences, Geosciences and Biosciences, Office of Basic Energy Sciences, US Department of Energy under contract DE-AC05-00OR22725, Oak Ridge National Laboratory, managed and operated by UT-Battelle, LLC. The authors would also like to thank Drs. James S. Bogard, Juske Horita, Donald A. Palmer and David J. Wesolowski, all of who helped us to acquire some of the experimental equipment needed for this project and provided useful technical advice. Reviews by Dr. Sumit Chakraborty and an anonymous reviewer were also helpful.

APPENDIX A. SUPPLEMENTARY DATA

Supplementary data associated with this article can be found, in the online version, at doi:10.1016/j.gca.2009.02.035.

REFERENCES

Anovitz L. M., Elam J. M., Riciputi L. R. and Cole D. R. (1999) The failure of obsidian-hydration-dating: sources, implications, and new directions. *J. Archaeol. Sci.* **26**(7), 735–752.

Anovitz L. M., Elam J. M., Riciputi L. R. and Cole D. R. (2004) Isothermal time-series determination of the rate of diffusion of water in Pachuca obsidian. *Archaeometry* **46**, 301–326.

Anovitz L. M., Riciputi L. R., Cole D. R., Elam J. M. and Gruszkiewicz M. S. (2006a) The effect of changes in relative humidity on the hydration rate of Pachuca obsidian. *J. Non-Cryst. Solid.* **352**, 5652–5662.

Anovitz L. M., Cole D. R. and Fayek M. (2008) Mechanisms of rhyolitic glass hydration below the glass transition. *Am. Mineral.* **93**(7), 1166–1178.

Anovitz L. M., Riciputi L. R., Cole D. R., Fayek M. and Elam J. M. (2006b) Obsidian hydration: a new paleothermometer. *Geology* **34**(7), 517–520.

Cobean R. H., Vogt J. R., Glasscock M. D. and Stocker T. L. (1991) High-precision trace-element characterization of major Mesoamerican obsidian sources and further analyses of artifacts from San Lorenzo Tenochtitlan, Mexico. *Latin Am. Antiquity* **2**, 69–91.

Cohen P. (1980) Water coolant technology of power reactors. *Am. Nucl. Soc.*, 78.

Cruz R. (1994) Analysis arqueologico del yacimiento de obsidiana de Sierra Las Navajas, Hidalgo.

Cruz R. and Pastrana A. (1994) Sierra Las Navajas, Hidalgo: nuevas investigaciones sobre la explotacion pre-colonial de obsidiana. *Simposium sobre arqueologia en el estado de Hidalgo, trabajos recientes* **1989**, 31–45.

Dingwell D. B., Romano C. and Hess K. U. (1996) The effect of water on the viscosity of a haplogranitic melt under P-T-X conditions relevant to silicic volcanism. *Contrib. Mineral. Petrol.* **124**(1), 19–28.

Doremus R. H. (1995) Diffusion of water in silica glass. *J. Mater. Res.* **10**(9), 2379–2389.

Doremus R. H. (1996) Diffusion of oxygen in silica glass. *J. Electrochem. Soc.* **143**(6), 1992–1995.

Doremus R. H. (1998a) Comment on "Stationary and mobile hydrogen defects in potassium feldspar" by A.K. Kronenberg, R.A. Yund, G.R. Rossman. *Geochim. Cosmochim. Acta* **62**(2), 377–378.

Doremus R. H. (1998b) Diffusion of water and oxygen in quartz: reaction-diffusion model. *Earth Planet. Sci. Lett.* **163**(1–4), 43–51.

Friedman I., Evans C., Meighan C. W., Foote L. J. and Aiello P. V. (1968) Obsidian dating revisited. *Science* **162**(3855), 813.

Friedman I., Gleason J., Sheppard R. A., Gude A. J. R. (1993a) Deuterium fractionation as water diffuses into silicic volcanic ash. In *Climate Change in Continental Isotopic Records*, Vol. 78 (ed. P.K. Swart, Lohmann, K.C., McKenzie, J., Savin, S.). American Geophysical Union, pp.321–323.

Friedman I., Gleason J., Warden A. (1993b) Ancient climate from deuterium content of water in volcanic glass. In *Climate Change in Continental Isotopic Records*, Vol. 78 (ed. P.K. Swart, Lohmann, K.C., McKenzie, J., Savin, S.). American Geophysical Union, pp. 309–319.

Friedman I. and Smith R. L. (1959) Geochemical method for dating obsidian artifacts. *Science* **129**(3358), 1282–1290.

Friedman I. and Smith R. L. (1960) A new dating method using obsidian.1. The development of the method. *Am. Antiquity* **25**(4), 476–522.

Friedman I., Smith R. L. and Long W. D. (1966) Hydration of natural glass and formation of perlite. *Geol. Soc. Am. Bull.* **77**(3), 323.

Friedman I., Trembour F. (1980) *State-of-the-Art of Obsidian Hydration Dating*. Abstracts of Papers of the American Chemical Society 179 (MAR), 13-NUCL.

Friedman I. and Trembour F. (1983) Obsidian-hydration-dating update. *Am. Antiquity* **48**(3), 544–547.

García-Barcena J. (1975) Las minas de obsidiana de la Sierra Las Navajas, Hidalgo, Mexico. *Actas del XLI Congreso Internacional de Americanistas* **369**, 377.

Goranson R. (1931) The solubility of water in granitic magmas. *Am. J. Sci.* **22**, 481–502.

Holmes W. H. (1900) The obsidian mines of Hidalgo, Mexico. *Am. Anthropol.* **2**, 405–416.

Horita J., Cole D., Polyakov V. and Driesner T. (2002) Experimental and theoretical study of pressure effects on hydrogen isotope fractionation in the system brucite-water at elevated temperatures. *Geochim. Cosmochim. Acta* **66**(21), 3769–3788.

Lighthart L. A. (2001) The geology, petrology and geo-archaeology of Sierra Las Navajas, Hidalgo, Mexico. Ph. D, Tulane University.

Lindsay W. T. J. (1989) Chemistry of steam cycle solutions: principles. In *The ASME Handbook on Water Technology for Thermal Power Systems* (ed. P. Cohen). ASME (American Society of Mechanical Engineers), pp. 341–544.

Lopez-Agilar F., Nieta-Calleja, R., Cobean, R.H. (1989) La producción de obsidiana en al sierra as Navajas, Hidalgo. In *La obsidiana en Mesoamerica* (ed. M. A. C. Gaxiola, J.E.), pp. 193–197.

Lovell M., Dalgliesh R. M., Richardson R. M., Barnes A. C., Enderby J. E., Evans B. and Webster J. R. P. (1999) Depth of water incorporation intro float glass surfaces studied by neutron reflection. *Phys. Chem. Chem. Phys.* **1**, 2379–2381.

Mazer J. J., Stevenson C. M., Ebert W. L. and Bates J. K. (1991) The experimental hydration of obsidian as a function of relative-humidity and temperature. *Am. Antiquity* **56**(3), 504–513.

Pastrana A. (1996) La explotacion azteca de obsidiana en la Sierra Las Navajas. Master's, Escuala Nacional de Antropologia e Historia.

Richardson R., Dalgleish R. M., Brennan T., Lovell M. R. and Barnes A. C. (2001) A neutron reflection study of the effect of water on the surface of float glass. *J. Non-Cryst. Solid.* **292**, 93–107.

Riciputi L. R., Elam J. M., Anovitz L. M. and Cole D. R. (2002) Obsidian diffusion dating by secondary ion mass spectrometry: a test using results from Mound-65, Chalco, Mexico. *J. Archaeol. Sci.* **29**(10), 1055–1075.

Ridings R. (1996) Where in the world does obsidian hydration dating work? *Am. Antiquity* **61**(1), 136–148.

Stevenson C. M., Carpenter J. and Scheetz B. E. (1989) Obsidian dating – recent advances in the experimental-determination and application of hydration rates. *Archaeometry* **31**, 193–206.

Stolper E. (1982a) The speciation of water in silicate melts. *Geochim. Cosmochim. Acta* **46**(12), 2609–2620.

Stolper E. (1982b) Water in silicate-glasses – an infrared spectroscopic study. *Contrib. Mineral. Petrol.* **81**(1), 1–17.

Stolper E. (1989) Temperature-dependence of the speciation of water in rhyolitic melts and glasses. *Am. Mineral.* **74**(11–12), 1247–1257.

Tenorio D., Cabral A., Bosch P., Jimenez-Reyes M. and Bulbulian S. (1998) Differences in coloured obsidians from Sierra de Pachuca, Mexico (Archaeology, pre-Hispanic Mexico, techniques). *J. Archaeol. Sci.* **25**(3), 229–234.

Tuttle O. F., Bowen N. L. (1958) Origin of granite in light of experimental studies in the system $NaAlSi_3O_8$-$KAlSi_3O_8$-SiO_2-H_2O. In *Geological Society of America. Memoir 74*. Geological Society of America, New York.

Zhang Y. X., Belcher R., Ihinger P. D., Wang L. P., Xu Z. J. and Newman S. (1997a) New calibration of infrared measurement of dissolved water in rhyolitic glasses. *Geochim. Cosmochim. Acta* **61**(15), 3089–3100.

Zhang Y. X., Jenkins J. and Xu Z. J. (1997b) Kinetics of the reaction $H_2O + O = 2OH$ in rhyolitic glasses upon cooling: geospeedometry and comparison with glass transition. *Geochim. Cosmochim. Acta* **61**(11), 2167–2173.

Zhang Y. X., Stolper E. M. and Wasserburg G. J. (1991) Diffusion of water in rhyolitic glasses. *Geochim. Cosmochim. Acta* **55**(2), 441–456.

Zhang Y. X., Xu Z. J. and Liu Y. (2003) Viscosity of hydrous rhyolitic melts inferred from kinetic experiments, and a new viscosity model. *Am. Mineral.* **88**(11–12), 1741–1752.

Associate editor: Thomas Chacko